Raman spectra and structure of amorphous Si

R. L. C. Vink*
Instituut Fysische Informatica, Utrecht University, Princetonplein 5, 3584 CC Utrecht, The Netherlands

G. T. Barkema
Theoretical Physics, Utrecht University, Princetonplein 5, 3584 CC Utrecht, The Netherlands

W. F. van der Weg
Debye Institute, Utrecht University, P.O. Box 80000, 3508 TA Utrecht, The Netherlands
(Received 16 May 2000; published 2 March 2001)

In 1985, Beeman, Tsu, and Thorpe established an almost linear relation between the Raman transverse-optic (TO) peak width Γ and the spread in mean bond angle $\Delta\theta$ in a-Si. This relation is often used to estimate the latter quantity in experiments. In the last decade, there has been significant progress in the computer generation of sample networks of amorphous silicon. Exploiting this progress, this paper presents a more accurate determination of the relation between Γ and $\Delta\theta$ using 1000-atom configurations. Also investigated and quantified are the relations between the TO peak frequency and the ratio of the intensities of the transverse-acoustic (TA) and TO peaks, both as functions of $\Delta\theta$. As $\Delta\theta$ decreases, the TA/TO intensity ratio decreases and the TO peak frequency increases. These relations offer additional ways to obtain structural information on a-Si from Raman measurements.

DOI: 10.1103/PhysRevB.63.115210 PACS number(s): 61.43.Dq, 61.43.Bn, 63.50.+x, 78.30.Ly

I. INTRODUCTION

Many structural properties of a-Si, such as defect concentration and variation in mean bond angle, are difficult to determine experimentally. This is because it is impossible to measure directly the coordinates of atoms in a-Si. However, important information on the structure of a-Si can be obtained indirectly through a number of experimental techniques. These techniques include neutron, x-ray, and Raman scattering, electron-spin resonance, and x-ray photoabsorption. We focus here on Raman measurements, which are relatively easy to perform and frequently used to obtain structural information about the amorphous network.[1–4]

The experimental Raman spectra of a-Si show two distinct bands, at about 150 and 480 cm^{-1}, associated with transverse-acoustic (TA) and transverse-optic (TO) vibrational modes, respectively. Certain features in the Raman spectrum are highly sensitive to the structural properties of the a-Si sample. For example, the width of the TO band is related to the root-mean-square bond-angle variation $\Delta\theta$ in the amorphous network.[5]

In several computational studies,[6–8] the relation between Γ and $\Delta\theta$ was quantified. All studies indicate a broadening of the TO peak with increasing $\Delta\theta$, but there is no quantitative agreement. The linear relation of Beeman, Tsu, and Thorpe $\Gamma = 15 + 6\Delta\theta$, which dates back to 1985, is often used by experimentalists to determine $\Delta\theta$ from Raman measurements. Here, Γ is in cm^{-1} and $\Delta\theta$ in degrees.

Beeman, Tsu, and Thorpe derived his relation using nine structural models of a-Si. Of these models, five were generated from the same 238-atom, hand-built model by Connell and Temkin,[9] which contains only even-membered rings. In contrast, all simulations on a-Si find an abundance of fivefold and sevenfold rings. Moreover, these five Connell-Temkin models are statistically dependent and not periodic, consequently containing a large fraction of surface atoms. Experimental values of $\Delta\theta$, based on the radial distribution function of a-Si obtained in neutron-diffraction studies, range from 9.9° to 11.0°.[10] Of the nine structural models used by Beeman, only three exhibit values of $\Delta\theta$ in this range. New techniques to generate a-Si structures, such as the activation-relaxation technique (ART),[11–13] as well as more powerful computers, have made it possible to generate larger and more realistic a-Si systems via computer simulation.

Also the description of the Raman scattering process has improved. Beeman used the bond-polarizibility model proposed by Alben *et al.*,[14] which dates back to 1975. Characteristic for this model is the inclusion of three weighting parameters whose values must be set somewhat arbitrarily. Several studies have indicated that the values originally proposed by Alben *et al.* yield an incorrect value for the depolarization ratio.[3,4] These studies therefore propose different weights. Since then, other polarizibility models have been proposed, for example, by Marinov and Zotov.[15]

In this paper, we will reinvestigate the relation between Γ and $\Delta\theta$ by computer simulation. This simulation is based on a large number of 1000-atom, periodic configurations with structural properties (radial distribution function, spread in mean bond angle) that are in excellent agreement with experiment. Furthermore, recent advances in neutron scattering techniques have made it possible to directly compare the bond-polarizability models to experiment.[16] We therefore also include a detailed comparison of the model of Alben *et al.* and the model of Marinov and Zotov to experiment.

Additionally, we present two other methods to obtain structural information from the Raman spectrum. The TA/TO intensity ratio[1] and the location of the TO peak[17] are believed to be directly related to $\Delta\theta$; these relations will be quantified.

The outline of this paper is as follows. In Sec. II, we explain the generation of the *a*-Si configurations used in this study. We then discuss how the Raman spectrum is obtained from these configurations. The results and conclusions are presented in Secs. III and IV, respectively.

II. METHOD

To calculate Raman spectra, three ingredients are required: (1) a potential describing the atomic interactions in the sample, (2) a continuous random network representing a realistic sample of *a*-Si, and (3) a model assigning Raman activities to the vibrational eigenmodes of the sample.

In the present work, we use a modified version of the Stillinger-Weber (SW) potential for all calculations. This potential has the same functional form as the original SW potential,[18] but with different parameters. The parameters were chosen specifically to describe *a*-Si, see Ref. 19.

A. Sample generation

To study the effect of $\Delta\theta$ on the Raman spectrum, we require a number of *a*-Si configurations with varying values of $\Delta\theta$. These configurations were generated using the ART.[11–13] As was shown in previous studies,[11,12] the ART yields structures in good agreement with experiment. They display a low density of coordination defects, a narrow bond-angle distribution, and an excellent overlap with the experimental radial distribution function (RDF). The method is outlined below.

(1) Initially, 1000 atoms are placed at random in a periodic cubic cell; the configuration is then relaxed at zero pressure.

(2) The configuration is annealed using the ART. One ART move consists of two steps: (1) the sample is brought from a local-energy minimum to a nearby saddle-point (activation; and (2) then relaxed to a new minimum with a local-energy minimization scheme including volume optimization at zero pressure. The new minimum is accepted with a Metropolis probability at temperature $T=0.25$ eV.

(3) Every 50 ART moves, up to approximately five ART moves per atom when the energy has reached a plateau, the configuration is stored. For 1000-atom samples, this procedure yields a set containing 100 samples.

This procedure is repeated nine times generating nine statistically independent sets of 100 correlated configurations each. For each set, we found that $\Delta\theta$ ranges from approximately 10° for the well-annealed configurations, to approximately 14° for the poorly annealed configurations.

B. Calculation of Raman spectra

We focus on the reduced Raman spectrum $I(\omega)$ with thermal and harmonic oscillator factors removed. This spectrum is a function of frequency ω and of the form

$$I(\omega)=C(\omega)g(\omega), \tag{1}$$

where $g(\omega)$ is the vibrational density of states (VDOS) and $C(\omega)$ is a coupling parameter, which depends on frequency and on the polarization horizontal-horizontal (HH) or horizontal-vertical (HV) of the incident light used in the Raman experiment.

To calculate the VDOS, the Hessian is calculated. Diagonalization of the Hessian gives the frequencies of the vibrational modes from which the VDOS is obtained.

The function $C(\omega)$ is obtained from the polarizibility tensor $\alpha(\omega)$. In terms of $\alpha(\omega)$, the coupling parameter for HH and HV Raman scattering becomes $C_{\mathrm{HH}}(\omega_p)=7G^2+45A^2$ and $C_{\mathrm{HV}}(\omega_p)=6G^2$, respectively, with A and G^2 given by the tensor invariants

$$A=\tfrac{1}{3}\left[\alpha_{11}+\alpha_{22}+\alpha_{33}\right] \tag{2}$$

and

$$G^2=3[\alpha_{12}^2+\alpha_{23}^2+\alpha_{31}^2]+\tfrac{1}{2}\left[(\alpha_{11}-\alpha_{22})^2+(\alpha_{22}-\alpha_{33})^2+(\alpha_{33}-\alpha_{11})^2\right], \tag{3}$$

see for instance Ref. 20.

The form of the polarizibility tensor $\alpha(\omega)$ still needs to be specified; this is the most uncertain part of the calculation. Several models have been proposed, amongst which are the commonly used model of Alben *et al.*[14] and the more recent model of Marinov and Zotov.[15]

In the model of Alben *et al.*, a cylindrical symmetry of the individual bonds is assumed and each bond is treated independently as a homopolar, diatomic molecule. Three different forms for the bond polarizibility tensor are introduced,

$$\alpha_1(\omega_p)=\sum_{l,\Delta}\vec{u}_l\cdot\vec{r}_\Delta[\vec{r}_\Delta\vec{r}_\Delta-\tfrac{1}{3}\mathbf{I}], \tag{4}$$

$$\alpha_2(\omega_p)=\sum_{l,\Delta}\vec{u}_l\cdot\vec{r}_\Delta[\tfrac{1}{2}(\vec{r}_\Delta\vec{u}_l+\vec{u}_l\vec{r}_\Delta)-\tfrac{1}{3}\mathbf{I}], \tag{5}$$

$$\alpha_3(\omega_p)=\sum_{l,\Delta}(\vec{u}_l\cdot\vec{r}_\Delta)\mathbf{I}. \tag{6}$$

Here, the summation runs over all atoms l in the sample and their nearest neighbors Δ, $\vec{r}_\Delta$ is the unit vector from the equilibrium position of atom l to the nearest neighbor Δ, $\vec{u}_l$ is the displacement vector of atom l when it is vibrating in mode p, and $\mathbf{I}$ is the unit dyadic. The total polarizibility tensor α is a weighted sum of the three terms, i.e., $\alpha=B_1\alpha_1+B_2\alpha_2+B_3\alpha_3$. As was stated in the Introduction, the precise choice of the weights B is somewhat arbitrary and this is the major shortcoming of the model. Several studies have indicated that mechanisms 1 and 3 provide the main contribution to the Raman scattering process; these propose to use $B_1:B_2:B_3$ proportional to 2:0:1, respectively.[3,4] In this paper, we will use this set of weights.

The model of Marinov and Zotov (MZ) has no free parameters. In this model, the bond polarizibility is expressed as a sum of three components; two components parallel to the bond arising from bonding and nonbonding electrons and a third component perpendicular to the bond, see Ref. 15. Under these assumptions, the polarizibility tensor takes the form

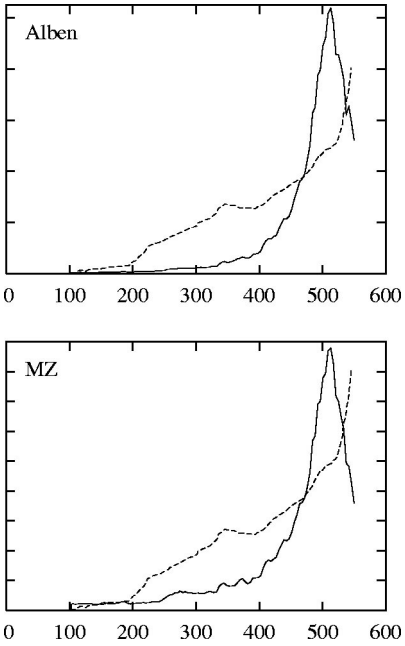

FIG. 1. HV Raman coupling parameter for a-Si calculated using the model of Alben *et al.* (top) and the MZ model (bottom). The dashed line is the experimental result taken from Ref. 16. Frequency is in cm^{-1} and all curves are area-normalized.

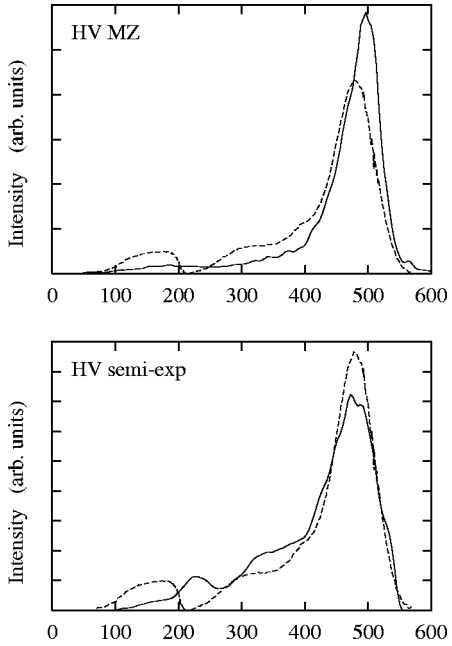

FIG. 2. Top: Reduced HV Raman spectrum for a-Si calculated using the MZ model (solid). Bottom: Reduced HV Raman spectrum calculated using the semiexperimental approach the VDOS is obtained by simulation, the coupling parameter is taken from Ref. 16. The dashed line in both graphs shows an experimental reduced Raman spectrum taken from Ref. 21. Frequency is in cm^{-1} and all spectra are area-normalized.

$$\alpha(\omega_p)=\sum_m r_m^2[(\vec{b}_m\cdot\vec{r}_m)\vec{r}_m\vec{r}_m+\tfrac{1}{2}(\vec{b}_m\vec{r}_m+\vec{r}_m\vec{b}_m)]. \quad (7)$$

Here, the summation runs over all bonds m in the sample, $\vec{r}_m$ is a unit vector parallel to the bond, r_m is the bond length, and $\vec{b}_m$ is defined as $\vec{u}_j-\vec{u}_i$; where $\vec{u}_i$ and $\vec{u}_j$ are the displacement vectors of atoms i and j constituting the mth bond, when vibrating in mode p. For a more detailed discussion on the differences between the two polarizibility models, see Ref. 15.

The coupling parameter for a-Si has also been determined experimentally[16] through neutron-scattering methods. According to this experiment, the coupling parameter is a slowly increasing function of frequency. We will use the experimental result of Ref. 16 to test the validity of both the model of Alben *et al.* and the MZ model.

III. RESULTS

First, in Sec. III A, we compare the polarizibility models of Alben *et al.* and Marinov and Zotov to experiment. In the subsequent sections, we investigate the relation between the spread in the bond angle $\Delta\theta$ and (1) Raman TO peak width, (2) Raman TO peak position, and (3) Raman TO/TA intensity ratio. We show results for HV-polarized light only; this is the usual experimental situation. Results for HH-polarized light have also been obtained and are available upon request.

A. Raman coupling parameter

The solid curves in Fig. 1 show the HV Raman coupling parameter for a-Si calculated using the model of Alben *et al.* (top) and the MZ model (bottom) for the bond polarizibility. The experimental result of Ref. 16 is also shown (dashed). For this calculation, we used a well-annealed, 1000-atom configuration with $\Delta\theta=10.0°$, since this will most closely resemble the experimental sample. We have checked that the general features of the curves in Fig. 1 do not depend on the details of the configuration used; a number of other well-annealed configurations with $\Delta\theta$ ranging from 10.0° to 11.0° gave similar results.

Figure 1 shows that both models yield an increasing coupling parameter for frequencies up to around 500 cm^{-1}. This is in qualitative agreement with experiment. For higher frequencies, the model calculations predict a sharp decrease in the coupling parameter. This is not confirmed by experiment.

The quantitative agreement with experiment is rather poor, especially in the low-frequency regime; both models provide substantially less activity in this regime than observed in experiment. For this reason, Raman spectra calculated using either of the two models yield TA peak amplitudes far below experimental values. This, in our opinion, is their major shortcoming.

This point is further illustrated in the top graph of Fig. 2, where we show the Raman spectrum calculated using the MZ model (solid) and an experimental spectrum (dashed) taken from Ref. 21. The experimental spectrum was obtained from ion-implanted a-Si which had been annealed at 500 °C for 2 h. Agreement between model and experiment, particularly in the low-frequency regime, is poor.

Given the overall poor performance of both the model of Alben *et al.* and the MZ model, it may be feasible to follow a semiexperimental approach in which a computer generated *a*-Si sample is used to calculate the VDOS and experimental data is used to describe the coupling parameter. This approach is justified because several studies have indicated that changes in the Raman spectrum of amorphous silicon are due to changes in the VDOS and upto a lesser degree to changes in the coupling parameter.[21,22]

It is important to recognize the limitations of this approach. The coupling parameter does to some extent depend on the structure of the sample. For example, in the limit of crystalline materials, the coupling becomes exactly zero for all frequencies, except for those in the TO band. However, no forbidden transitions arise in the disordered phase, which justifies the semiexperimental approach used here.

The results of the semiexperimental approach are illustrated in the bottom graph of Fig. 2. Here, we show the Raman spectrum obtained by multiplying a computer-generated VDOS with experimental coupling parameter data (solid). To calculate the VDOS, we used a well-annealed *a*-Si sample with $\Delta\theta = 10.0°$; the experimental coupling parameter was taken from Ref. 16. The dashed line shows again the experimental Raman spectrum taken from Ref. 21. Agreement with experiment has improved substantially.

Of the two models considered here, the MZ model provides slightly more activity in the low-frequency regime than the model of Alben *et al.*; comparison with experiment would therefore favor the MZ model. However, given the overall poor performance of both models, we will also show in the following sections results obtained using the semiexperimental approach.

B. Raman TO peak width vs $\Delta\theta$

The intensity of the Raman TO peak decreases abruptly on the high-frequency side, but not on the low-frequency side. Beeman therefore defines Γ as twice the half-width at half the maximum height on the high-frequency side of the TO peak, as a meaningful parameter to specify the TO peak width.[6] In this paper, we use the same definition.

The solid lines in Fig. 3 show the relation between Γ and $\Delta\theta$ for HV-polarized light, derived using the model of Alben *et al.* (top), the MZ model (middle), and the semiexperimental approach (bottom). Also shown is the result obtained by Beeman, Tsu, and Thorpe (dashed).

Both the model of Alben *et al.* and the MZ model produce similar results; linear least-square fits yield the equations $\Gamma/2 = 3.0\Delta\theta - 6.5$ and $\Gamma/2 = 3.7\Delta\theta - 13.3$, respectively. Compared to the result of Beeman, Tsu, and Thorpe, $\Gamma/2 = 3.0\Delta\theta + 7.5$, we see agreement on the sensitivity (i.e., slope of the lines) of Γ to $\Delta\theta$, but not on the overall offset (i.e., intercepts of the lines). The same holds for the result obtained in the semiexperimental approach; least-square fitting yields $\Gamma/2 = 3.3\Delta\theta + 9.2$ in that case.

C. Raman TO peak position vs $\Delta\theta$

As another way to obtain structural information on *a*-Si from its Raman spectrum, we investigate the relation between the TO peak frequency (ω_{TO}) and $\Delta\theta$. Figure 4 shows the relation between ω_{TO} and $\Delta\theta$ for HV-polarized light, derived using the model of Alben *et al.* (top), the MZ model (middle), and the semiexperimental approach (bottom).

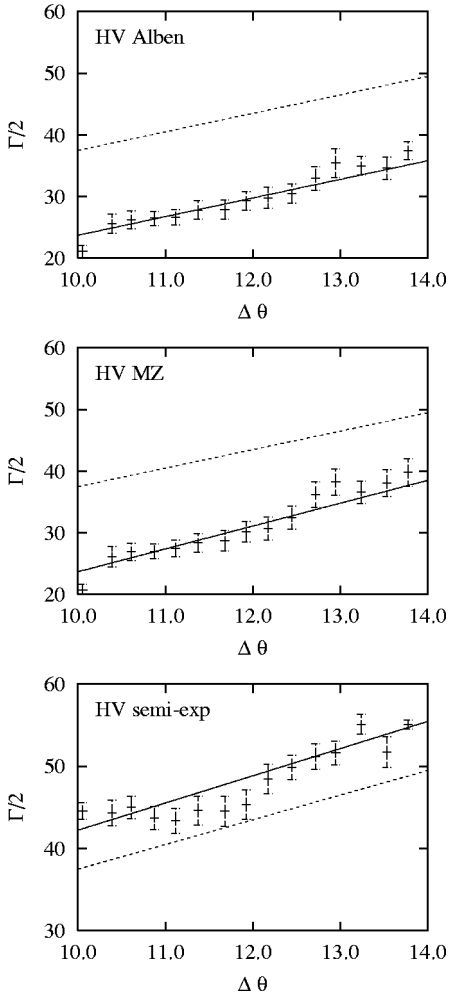

FIG. 3. HV Raman TO peak width $\Gamma/2$ as a function of $\Delta\theta$, calculated using the model of Alben *et al.* (top), the MZ model (middle), and the semiexperimental approach (bottom). The solid lines are linear least-squares fits; the dashed line is the result of Beeman, Tsu, and Thorpe, $\Gamma/2 = 7.5 + 3\Delta\theta$. The units of $\Gamma/2$ and $\Delta\theta$ are cm^{-1} and degrees, respectively.

According to Fig. 4, ω_{TO} shifts to higher frequency as $\Delta\theta$ decreases. However, agreement with experiment for both the model of Alben *et al.* and the MZ model is poor. Experimental Raman spectra of well-annealed *a*-Si samples yield ω_{TO} in the order of 480 cm^{-1}.[21] For well-annealed configurations, for which $\Delta\theta$ ranges from 9.9° to 11.0°, the models exceed the experimental value by around 20 cm^{-1}.

The semiexperimental approach is in much better agreement with experiment; a linear fit yields the equation $\omega_{TO} = -2.5\Delta\theta + 505.5$, which for $\Delta\theta = 10.0°$ leads to $\omega_{TO} = 480.5\ cm^{-1}$.

The cause of this is that in the model of Alben *et al.* and the MZ model, ω_{TO} is determined by the peak in the coupling parameter, whereas in the semiexperimental approach, it is determined by the VDOS.

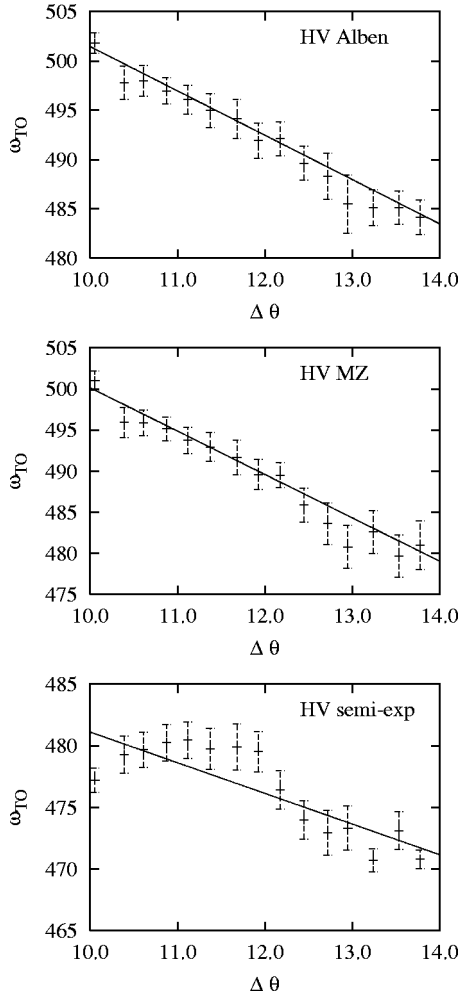

FIG. 4. Reduced HV Raman TO peak position as a function of $\Delta\theta$ for a-Si calculated using the model of Alben *et al.* (top), the MZ model (middle), and the semiexperimental approach (bottom). The peak position and $\Delta\theta$ are given in cm^{-1} and degrees, respectively. The solid lines are least-squares fits through the datapoints.

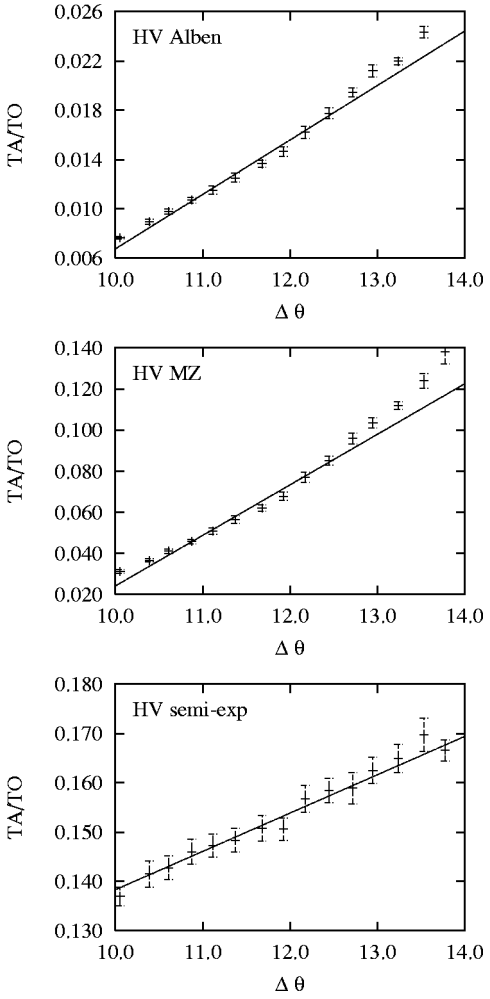

FIG. 5. HV Raman TA/TO intensity ratio as a function of $\Delta\theta$ for a-Si calculated using the model of Alben *et al.* (top), the MZ model (middle), and the semiexperimental approach (bottom). The solid lines are least-squares fits. $\Delta\theta$ is in degrees.

D. Raman TA/TO intensity ratio vs $\Delta\theta$

Next, we confirm that the TA/TO intensity ratio is directly related to $\Delta\theta$. Figure 5 shows the relation between reduced Raman TA/TO intensity and $\Delta\theta$ for HV-polarized light for the model of Alben *et al.* (top), the MZ model (middle), and the semiexperimental approach (bottom).

From Fig. 5, we see that the TA/TO intensity ratio increases with increasing $\Delta\theta$. The increase is approximately linear.

HV Raman experiments on well-annealed a-Si samples yield a reduced TA/TO intensity ratio around 0.11.[21] For both the model of Alben *et al.* and the MZ model, the HV TA/TO ratio is of order 10^{-2}, i.e., one order of magnitude below the experimental value. This is consistent with the earlier finding that both models underestimate the Raman activity in the low-frequency regime of the spectrum, see Sec. III A.

The semiexperimental approach, on the other hand, yields a TA/TO ratio of 0.14 for $\Delta\theta = 10.0°$ in better agreement with experiment.

IV. CONCLUSIONS

We have generated nine independent sets of 1000-atom samples of a-Si that display a variety of short-range orders; the spread in nearest-neighbor bond angles ranges from 10° to 14°. For these samples, the HV Raman spectra are calculated. To describe the Raman scattering process, we have used the earlier bond-polarizibility model of Alber *et al.*, the more recent model of Marinov and Zotov, as well as experimental data taken from Ref. 16.

Comparison to experiment shows that both the model of Alben *et al.* and the MZ model greatly underestimate the Raman activity in the low-frequency regime of the spectrum. This makes these models less suitable to describe low-frequency features of the Raman spectrum, for instance, the TA peak. Of the two models considered here, the MZ model is closer to experiment. However, for a more accurate calculation of Raman spectra, we propose a semiexperimental approach. In this approach, the VDOS is obtained in computer simulation and experimental data is used to describe the coupling parameter.

As ways to obtain structural information on a-Si from its

Raman spectrum, we have investigated the relation between the TO peak width Γ and $\Delta\theta$, as well as the relations between the TO peak frequency and the TA/TO intensity ratio as functions of $\Delta\theta$.

According to our results, where we used the semiexperimental approach, Γ and $\Delta\theta$ are related by $\Gamma/2=3.3\Delta\theta+9.2$ for HV-polarized light. Here, Γ is in cm^{-1} and $\Delta\theta$ in degrees. Comparing this to the result of Beeman, Tsu, and Thorpe ($\Gamma/2=3\Delta\theta+7.5$), we find that our result is similar.

Our results also show a shift of the Raman TO peak frequency (ω_{TO}) towards higher frequency as $\Delta\theta$ decreases. In the semiexperimental approach, a linear least-square fit yields $\omega_{TO}=-2.5\Delta\theta+505.5$ for HV-polarized light. Here, ω_{TO} is in cm^{-1} and $\Delta\theta$ in degrees. According to this equation, the shift of ω_{TO} is approximately 7.5 cm^{-1}, going from unannealed a-Si ($\Delta\theta\approx13°$) to annealed a-Si ($\Delta\theta\approx10°$). This is in quantitative agreement with experiment.[21]

Finally, we have shown that the reduced Raman TA/TO intensity ratio (I) is directly related to $\Delta\theta$; I decreases linearly with decreasing $\Delta\theta$. Using the semiexperimental approach, we obtain the relation $I=0.0078\Delta\theta+0.0606$, where $\Delta\theta$ is in degrees.

*Email address: vink@phys.uu.nl

[1] N. Maley, D. Beeman, and J. S. Lannin, Phys. Rev. B **38**, 10 611 (1988).
[2] J. E. Smith, Jr., M. H. Brodsky, B. L. Crowder, and M. I. Nathan, Phys. Rev. Lett. **26**, 642 (1971).
[3] D. Bermejo and M. Cardona, J. Non-Cryst. Solids **32**, 405 (1979).
[4] M. Ivanda, O. Gamulin, and W. Kiefer, J. Mol. Struct. **480–481**, 651 (1998).
[5] W. C. Sinke, S. Roorda, and F. W. Saris, J. Mater. Res. **3**, 1201 (1988).
[6] D. Beeman, R. Tsu, and M. F. Thorpe, Phys. Rev. B **32**, 874 (1985).
[7] R. Tsu, J. G. Hernandez, and F. H. Pollak, J. Non-Cryst. Solids **66**, 109 (1984).
[8] C. K. Wong and G. Lucovsky, in *Materials Issues in Amorphous-Semiconductor Technology* edited by D. Adler, Y. Hamakawa, and A. Madan (Materials Research Society, Pittsburgh, 1986), p. 77.
[9] G. A. N. Connell and R. J. Temkin, Phys. Rev. B **9**, 5323 (1974).
[10] J. Fortner and J. S. Lannin, Phys. Rev. B **39**, 5527 (1989).
[11] G. T. Barkema and N. Mousseau, Phys. Rev. Lett. **77**, 4358 (1996).
[12] N. Mousseau and G. T. Barkema, Phys. Rev. E **57**, 2419 (1998).
[13] N. Mousseau and G. T. Barkema, Comput. Sci. Eng. **1**, 74 (1999).
[14] R. Alben, D. Weaire, J. E. Smith, Jr., and M. H. Brodsky, Phys. Rev. B **11**, 2271 (1975).
[15] M. Marinov and N. Zotov, Phys. Rev. B **55**, 2938 (1997).
[16] Fang Li and Jeffrey S. Lannin, Phys. Rev. B **39**, 6220 (1989).
[17] N. Zotov, M. Marinov, N. Mousseau, and G. T. Barkema, J. Phys. Condens. Matter **11**, 9647 (1999).
[18] F. H. Stillinger and T. A. Weber, Phys. Rev. B **31**, 5262 (1985).
[19] R. L. C. Vink, G. T. Barkema, W. F. van der Weg, and Normand Mousseau, J. Non-Cryst. Solids (to be published).
[20] R. J. Bell and D. C. Hibbins-Butler, J. Phys. C: Solid State Phys. **9**, 2955 (1976), and references therein.
[21] W. F. van der Weg, A. J. M. Berntsen, F. W. Saris, and A. Polman, Mater. Chem. Phys. **46**, 140 (1996).
[22] N. Maley and J. S. Lannin, Phys. Rev. B **35**, 2456 (1987).